



Universiteit
Leiden
The Netherlands

Mapping and ablation of atrial tachyarrhythmias : from signal to substrate

Groot, N.M.S. de

Citation

Groot, N. M. S. de. (2006, September 14). *Mapping and ablation of atrial tachyarrhythmias : from signal to substrate*. Retrieved from <https://hdl.handle.net/1887/4915>

Version: Corrected Publisher's Version

License: [Licence agreement concerning inclusion of doctoral thesis in the Institutional Repository of the University of Leiden](#)

Downloaded from: <https://hdl.handle.net/1887/4915>

Note: To cite this publication please use the final published version (if applicable).

chapter

8

Epicardial Multi-Site High Density Mapping As A New Approach to Identify The Substrate of Atrial Fibrillation

Natasja MS de Groot

Robert Klautz, Jerry Braun, Richard M. Houben

Martin J. Schalij, Maurits A. Allessie



Abstract

Introduction: Fractionated electrograms may be indicators of the arrhythmogenic substrate perpetuating atrial fibrillation (AF). The goal of this study was to evaluate a new epicardial multi-site high density mapping approach for assessing intra-atrial differences in fractionation characteristics of fibrillation potentials recorded during chronic AF (CAF) and to determine whether there are predilection sites for fractionation to occur.

Methods: Epicardial mapping was performed during cardiac surgery for mitral valve disease in patients with CAF ($n = 7$, 54 ± 6 yrs). The entire right and left atria were mapped with a 1 cm^2 electrode containing 60 unipolar electrodes (inter-electrode distance 1.5 mm). At each site, episodes of 10 seconds were analyzed. Regional differences in median AFCL, the incidence of fractionated potentials (F) and fractionation duration (time between the steepest negative deflection of the first and last component) were evaluated.

The incidence and degree of fractionation was related with the incidence of conduction block (CB) and conduction anisotropy (CA).

Results: Recordings were acquired from 24 ± 4 (20-32) mapping sites. Median AFCL ranged from 142 to 342 (201 ± 34 ms). The averaged degree of fractionation and fractionation delay was respectively 17 ± 13 (0-51)% and 23 ± 19 (6-44)ms. The incidence of fractionation was highest in the pulmonary vein area ($25 \pm 11\%$, $p = 0.02$). Fractionation was related with conduction block ($r = 0.86$, $p = 0.001$) and conduction anisotropy ($r = 0.30$, $p = 0.001$). Fractionation duration was only associated with conduction block ($r = 0.67$, $p = 0.001$) not with conduction anisotropy ($r = 0.21$, $p = 0.04$).

	AFCL (ms)	F (%)	FD (ms)	CB (%)	CA
intra-atrial variation	47 ± 44	36 ± 8	27 ± 5	19 ± 5	1.53 ± 0.53
inter-individual variation	133 ± 39	40 ± 7	34 ± 5	24 ± 9	1.62 ± 0.55

Conclusion: Intra-atrial variation and inter-individual variation in the spatial distribution of the degree of fractionation indicates that AF treatment needs to be individualized and emphasizes the need for an electrogram guided ablation approach. Epicardial multi-site, high density fractionation mapping as presented in this study might therefore become an important tool for identification and subsequent ablation of the arrhythmogenic substrate of AF in patients with mitral valve disease.

Introduction

AF can be the result of a variety of different mechanisms like multiple wavelets, single/multiple foci or a mother wave with passive daughter waves.^{1;2} Knowledge of these different mechanisms of AF is of paramount importance for selection of an appropriate treatment modality.

Treatment of AF consists besides medication nowadays mainly of focal ablation of (non) pulmonary vein triggers or isolation of the pulmonary veins.^{3;4} However, a recent study provided evidence that not only ablation or isolation of the *trigger* but also ablation of the arrhythmogenic *substrate* may eliminate AF. Nademanee et al. showed that ablation of areas of fractionated fibrillation potentials terminated AF.⁵ This finding suggests that fractionated electrograms may be indicators of the arrhythmogenic substrate responsible for the perpetuation of AF.

It is most likely that there is a large inter-individual variation in the location of the arrhythmogenic substrate. This could be the result of different underlying cardiac diseases in patients with AF. In addition, the degree of electrical and structural remodeling affecting atrial tissue may also vary between patients and there can be regional differences in the severity of remodeling. Hence, multi-site high density mapping of the entire atria during AF may be mandatory for localizing the arrhythmogenic substrate.

In chapter 6, fractionation characteristics of right atrial fibrillation potentials recorded during induced atrial fibrillation in patients with normal atria and during chronic AF in patients with valvular heart disease were compared. Fractionation fingerprints – providing information on the degree and duration of fractionation – differed between patients with acute and chronic AF. It was therefore proposed that fractionation fingerprints could be used to distinguish different types of AF and also to identify the substrate perpetuating AF.

The goal of the present study was to evaluate a new epicardial multi-site high density mapping approach for assessing intra-atrial differences in fractionation characteristics of fibrillation potentials and to determine whether there are predilection sites for fractionation to occur. For this purpose, the entire right and left atria and Bachmann's bundle were mapped during chronic atrial fibrillation (CAF) in patients with mitral valve disease.

Methods

Study Population

Intra-operative mapping of the atria was performed in patients with CAF ($n = 7$, 64 ± 13 (46-82) yrs, 4 male) prior to cardiac surgery for mitral valve disease and/or isolation of the pulmonary veins. All patients had permanent AF lasting more than one year (range 1 to 9 years). Underlying heart diseases were mitral valve disease in all patients. Left atrial diameter as measured with M-mode echocardiography was 4.9 ± 1.5 (2.9-7.6) cm. Anti-arrhythmic drugs were discontinued prior to cardiac surgery; none of the subjects had used amiodarone.

214

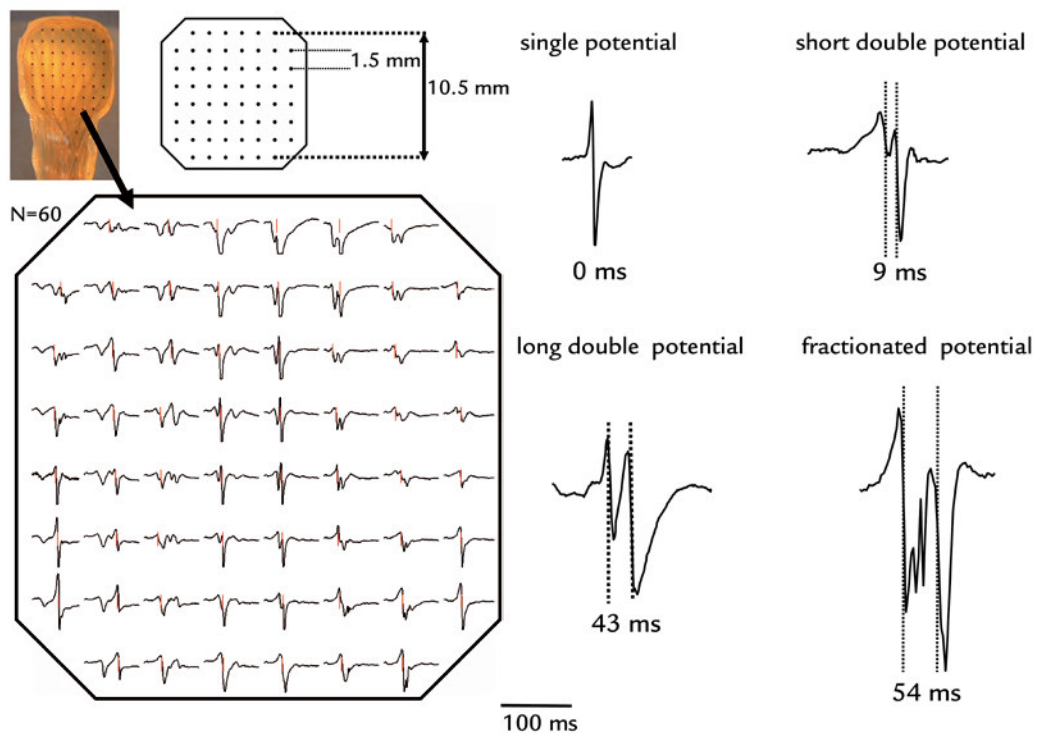


Figure 1.

Left panel: the mapping array consisted of 60 unipolar electrodes with a diameter of $0.3 \mu\text{m}$ and inter-electrode distance of 1.5 mm. *Right panel:* All fibrillation potentials recorded during 10 seconds of AF were classified as single, short double \rightarrow , long double \rightarrow , or fractionated potentials. In case of a double or fractionated potential, the duration of the potential (fractionation duration) was measured by determining the time between the steepest negative deflection of the first and last component.

Mapping procedure

AF was present at the moment of cardiac surgery in all patients. Mapping studies were performed before commencement to extra-corporal circulation. A small electrode was used for epicardial mapping of the atria (left panel Figure 1). This electrode contains 60 unipolar teflon-coated silver electrodes with a diameter of $0.3 \mu\text{m}$ and an inter-electrode distance of 1.5 mm . The electrode is attached to the index finger of the surgeon and positioned on the epicardium, thereby covering an area with a diameter of 10.5 mm . In this way, multiple sites at the right and left atria and Bachmann's bundle were sequentially mapped according to several imaginary 'lines' (Figure 2). The electrode was shifted along these lines thereby trying to avoid omission of areas at the expense of possible overlap between successive mapping sites.

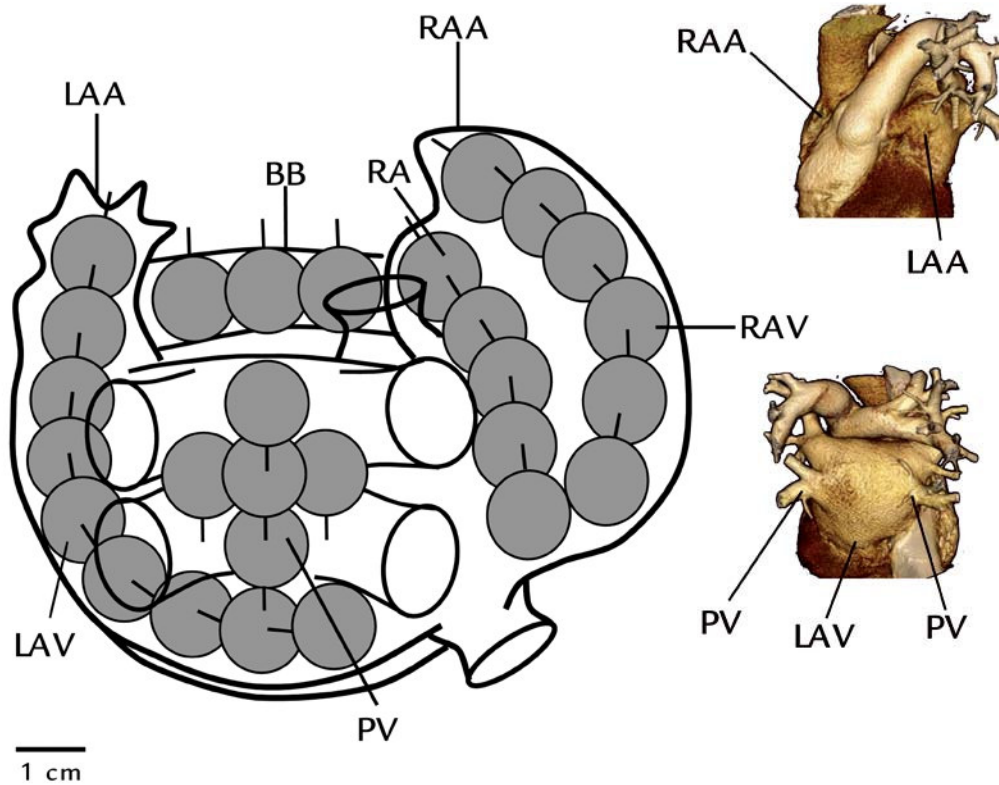


Figure 2.

Multiple sites at the right and left atria and Bachmann's bundle were sequentially mapped according to several imaginary 'lines.' The position and orientation of the mapping electrode along every mapping line is shown.

RAA = right atrial appendage, RAV = right atrioventricular groove, BB = Bachmann's bundle, LAA = left atrial appendage, PV = pulmonary vein area, LAV = left atrioventricular groove.

In the right atrium, mapping was performed from the cavotricuspid isthmus via the most lateral part of the right atrial free wall to the sinus node area (*RA-line*) and from the cavotricuspid isthmus parallel to the atrioventricular groove towards the right atrial appendage (*RAV-line*). In the left atrium, mapping was performed 1) along the left atrioventricular groove from the coronary sinus os towards the left atrial appendage (*LAV-line*), 2) from the middle of the atrioventricular groove at the posterior wall up to the sinus transversus fold and from the right pulmonary veins towards the left pulmonary veins (*pulmonary veins (PV)-lines*). Bachmann's bundle was mapped from the superior cavoatrial junction to the base of the left atrial appendage (*BB-line*).

The orientation of the electrode at every position at these lines was fixed, as shown in **Figure 2**. At each site, 60 electrograms were simultaneously acquired during 10 seconds of AF using a computerized mapping system.

A silver plate positioned inside the thoracic cavity served as an indifferent electrode. Unipolar epicardial fibrillation electrograms and the surface ECG were stored on hard disk after amplification (gain 1000), filtering (bandwidth 1-500 Hz), sampling (1 KHz) and analogue to digital conversion (12 bits).

Data Analysis

Fibrillation maps were off-line constructed with specialized mapping software as described in chapter 2.

The moment of local activation at each electrode was detected by automatically marking the steepest negative deflection of fibrillation potentials. AF cycle length (AFCL) was determined by measuring the time between activations by consecutive fibrillation waves. Median AFCL was assessed from fibrillation intervals recorded by all 60 unipolar electrodes during 10 seconds of AF.

Fibrillation potentials were classified according to the criteria described in chapter 6. At each mapping site, the incidence of single -, short double -, long double -, fractionated potentials and continuous electrical activity was determined. In case of a fractionated fibrillation potential or continuous electrical activity, the total duration (fractionation duration), defined as the time between the steepest negative deflection of the first and last component, was measured.

The incidence of fractionated potentials at each mapping site was related with the incidence of conduction block and conduction anisotropy. Local conduction block was defined as an inter-electrode conduction time ≥ 20 ms, corresponding with a conduction velocity ≤ 7.5 cm/s. To estimate the degree of conduction anisotropy, local conduction velocity vectors were determined in areas of 3x3 electrodes (3x3 mm). An ellipse was fitted through a collection of local conduction velocity vectors obtained during 10 seconds of AF. The ratio between the long and short axis of the ellipse, - thereby excluding conduction velocities ≤ 7.5 cm/s - was used as a measure of local conduction anisotropy.

A more detailed description of measurements of conduction anisotropy has been given in chapter 3.

Statistical Analysis

All data are expressed as mean \pm standard deviation, range or percentage. Students T-tests were used to evaluate intra-atrial differences in fractionation, fractionation duration, median AFCL. Pearson's correlation coefficient (r) was used to study the relation between the degree of fractionation, fractionation duration, AFCL, incidence of conduction block and conduction anisotropy. A probability level of 5% was considered statistically significant.

Table 1. Electrophysiological characteristics of the different mapping sites.						
		RA-line average/SD	RAV-line average/SD	BB-line average/SD	LAV-line average/SD	PV-line average/SD
1	AFCL (ms)	224 ± 7	186 ± 36	223 ± 8	232 ± 4	226 ± 48
	F (%)	5 ± 8	8 ± 6	2 ± 3	4 ± 4	14 ± 3
	FD (ms)	18 ± 11	30 ± 15	12 ± 2	18 ± 10	26 ± 15
	CT (%)	2 ± 3	5 ± 4	2 ±	6 ± 6	11 ± 0
	anisotropy	1.5 ± 0.5	1.3 ± 0.1	1.7 ± 0.3	1.1 ± 0.2	1.7 ± 0.2
2	AFCL (ms)		142	274 ± 50	237 ± 61	223 ± 44
	F (%)		22	4 ± 4	9 ± 9	21 ± 13
	FD (ms)		24	10 ± 4	15 ± 4	27 ± 3
	CT (%)		10	0 ± 1	5 ± 4	12 ± 5
	anisotropy		2.1	x	1.4 ± 0.4	1.5 ± 0.4
3	AFCL (ms)	183 ± 9	178 ± 16	195 ± 13	198 ± 15	
	F (%)	21 ± 9	27 ± 9	29 ± 12	6 ± 6	
	FD (ms)	25 ± 7	26 ± 5	20 ± 5	13 ± 4	
	CT (%)	9 ± 4	9 ± 3	14 ± 8	3 ± 4	
	anisotropy	1.6 ± 0.3	1.6 ± 0.4	1.7 ± 0.7	1.3 ± 0.3	
4	AFCL (ms)	156 ± 12	158 ± 4	165 ± 2	183 ± 14	181 ± 7
	F (%)	14 ± 4	19 ± 11	39 ± 17	25 ± 4	27 ± 11
	FD (ms)	23 ± 3	24 ± 8	31 ± 12	31 ± 8	22 ± 11
	CT (%)	9 ± 2	8 ± 5	15 ± 5	7 ± 6	8 ± 7
	anisotropy	1.7 ± 0.2	1.6 ± 0.3	3.0	1.6	2.0 ± 0.9
5	AFCL (ms)	192 ± 32	188 ± 11	189 ± 4	210 ± 33	221 ± 14
	F (%)	11 ± 6	14 ± 9	29 ± 8	7 ± 3	31 ± 9
	FD (ms)	26 ± 9	30 ± 9	28 ± 7	19 ± 5	31 ± 6
	CT (%)	6 ± 2	7 ± 3	16 ± 0.4	4 ± 3	16 ± 4
	anisotropy	1.6 ± 0.3	1.3 ± 0.1	1.9 ± 0.6	1.9 ± 1.0	1.8 ± 0.8
6	AFCL (ms)	223 ± 8	217 ± 13	174 ± 34	208 ± 5	
	F (%)	19 ± 16	12 ± 12	20 ± 27	32 ± 1	
	FD (ms)	34 ± 3	20 ± 8	26	34 ± 13	
	CT (%)	11 ± 6	6 ± 7	18 ± 26	26 ± 8	
	anisotropy	1.4 ± 0.1	1.3 ± 0.2	1.2	1.2 ± 0.0	
7	AFCL (ms)	190 ± 4	190 ± 11	217 ± 37	186	
	F (%)	36 ± 6	29 ± 9	26 ± 20	6	
	FD (ms)	28 ± 4	27 ± 4	30 ± 14	19	
	CT (%)	13 ± 3	12 ± 4	23 ± 13	2	
	anisotropy	1.3 ± 0.1	1.5 ± 0.2	2.1	1.2	

Results

Atrial Fibrillation Cycle Length

The cumulative frequency distribution of fibrillation intervals obtained from the right atrium, bachmann's bundle, the left atrioventricular groove and the left atrial posterior wall is shown in Figure 3. Each patient is represented by a different color. The interval histograms demonstrate an intra-atrial and inter-individual variation in fibrillation intervals. The averaged median AFCL determined from all mapping sites ranged from 142 ms to 342 (201 ± 34) ms and the intra-atrial variation of the median AFCL from 49 to 200 (92 ± 52) ms (Table 1). The inter-individual variation in AFCL was 133 ± 39 ms. There was no difference between the AFCL measured along the RA- (194 ± 27 ms) and the RAV-line (186 ± 26 ms, $p = 0.29$). The averaged median right atrial AFCL was significantly shorter than the averaged median left atrial AFCL (right atrium: 189 ± 26 ms versus left atrium: 211 ± 35 ms, $p < 0.001$). The shortest AFCL was measured in the right atrium ($n = 6$, right atrial appendage: $n = 2$, superior cavo-atrial junction: $n = 2$, right atrioventricular groove:

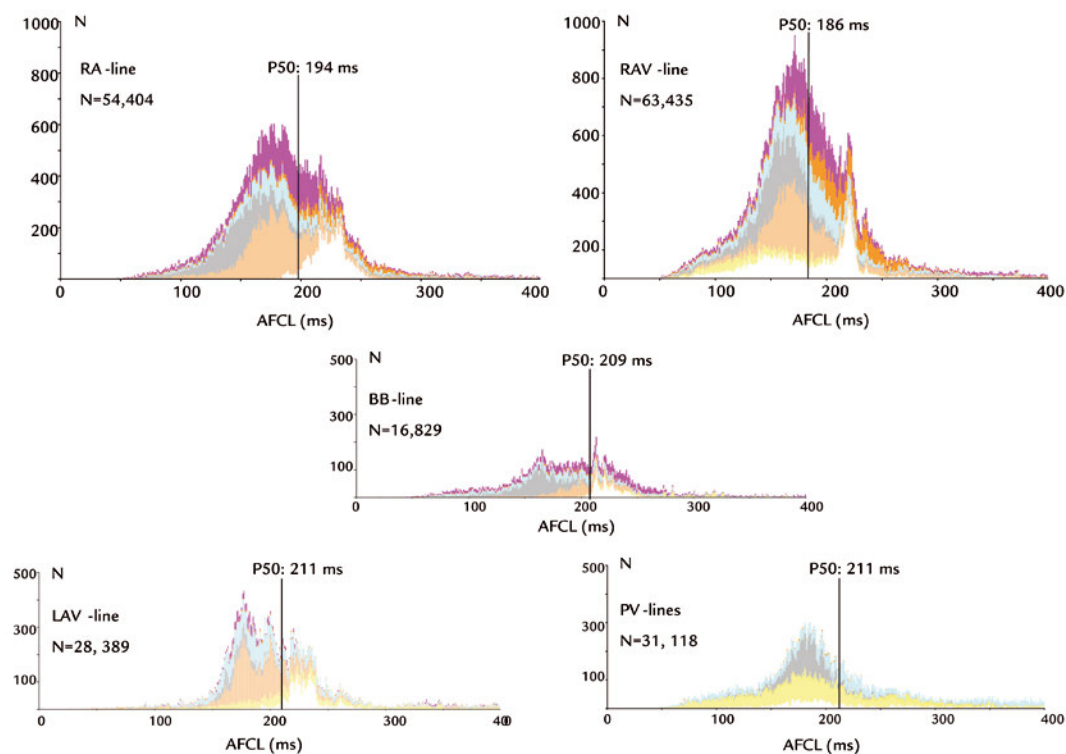


Figure 3.

The cumulative frequency distribution of fibrillation intervals recorded along the RA-, RAV-, BB-, LAV- and PV-lines. Each patient is represented by a different color.



Figure 4.

Examples of unipolar fibrillation electrograms recorded from the right atrial free wall (RAFW), bachmann's bundle (BB), the left atrial free wall (LAFW) and the pulmonary vein area (PV) obtained from one patient. Bars on the right indicate the proportion of single or short double potentials (white) and long double or fractionated potentials (grey).

$n = 2$) or at the left side of bachmann's bundle ($n = 1$). The longest AFCL was found in the right atrium (along the RAV-line) in only one patient. In all other patients, the longest AFCL was recorded from the left atrium; along the LAV-line ($n = 4$), at the border of the right pulmonary veins ($n = 1$) or along the left side of bachmann's bundle ($n = 1$).

In all patients, electrical activity could not be recorded from one or more mapping sites, despite assurance of good contact between atrial tissue and mapping electrode. These electrically silent areas were found along bachmann's bundle, the left atrioventricular groove or between the pulmonary veins.

Fractionation of Fibrillation Potentials

Figure 4 shows examples of unipolar fibrillation electrograms recorded from the right atrial free wall, bachmann's bundle, left atrial free wall and the pulmonary vein area obtained from one patient. Bars demonstrate the incidence of single or short double potentials (white) and long double potentials or fractionated potentials (grey) during

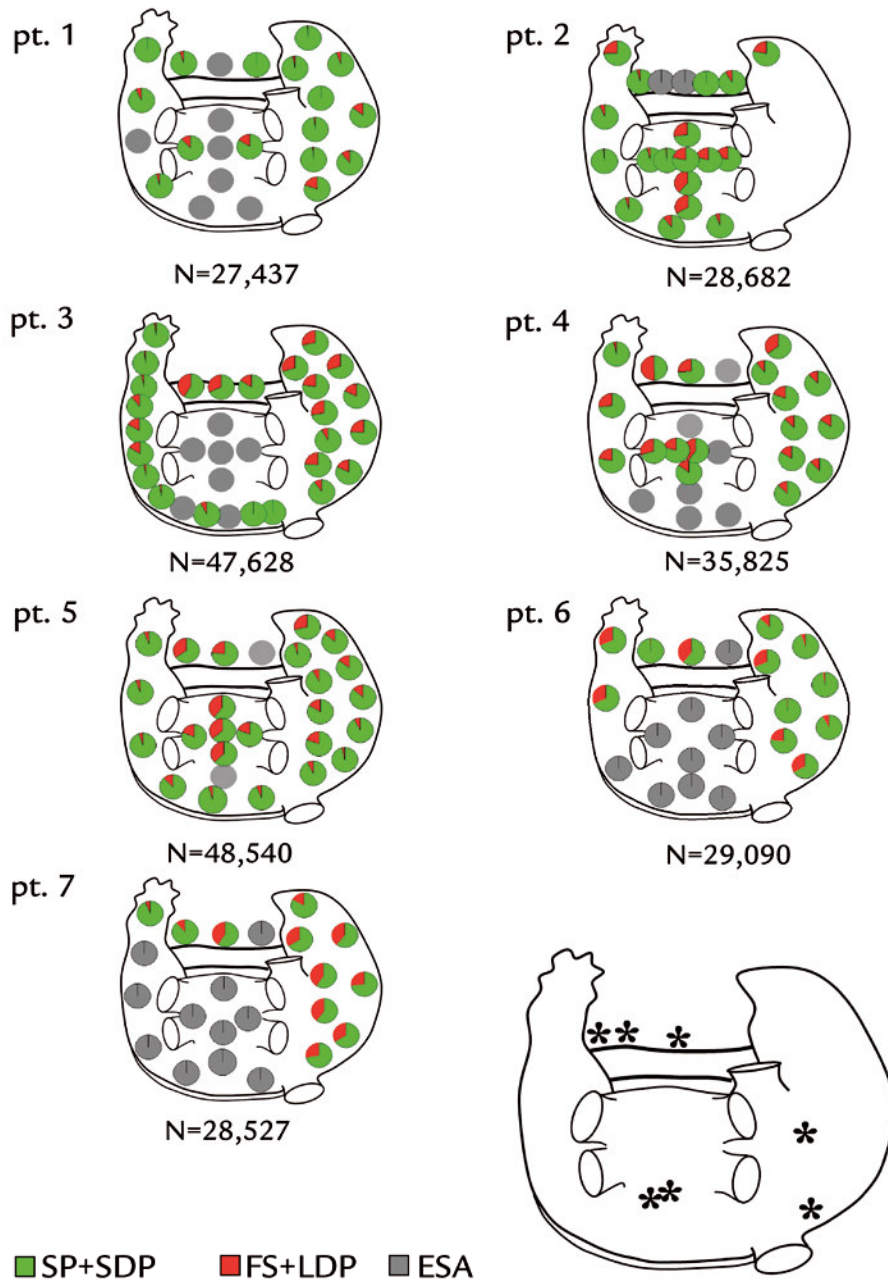


Figure 5. Mapping positions in every patient, demonstrating the proportion of single or short double potentials (green) and fractionated fibrillation potentials (red) at every mapping site. The number below the mapping scheme represents the total number of fibrillation potentials. SP: single potentials, SDP: short double potentials, LDP: long double potentials, FS: fractionated potentials, ESA: electrically silent areas. Lower right panel: summation of sites with the highest incidence of fractionated fibrillation potentials (asterisk).

10 seconds of AF at each of these sites. These recordings not only demonstrate a beat-to-beat variation in the morphology of fibrillation potentials, but also regional differences in the degree of fractionation.

Results of classification of fibrillation potentials at every mapping site for each patient are shown in Figure 5. Pies indicate the proportion of single or short double fibrillation potentials (green) and long double or fragmented potentials (red). Electrically silent areas are represented by grey circles. Surprisingly, the majority of fibrillation potentials at nearly all mapping sites consisted of single or short double potentials (Table 1); the

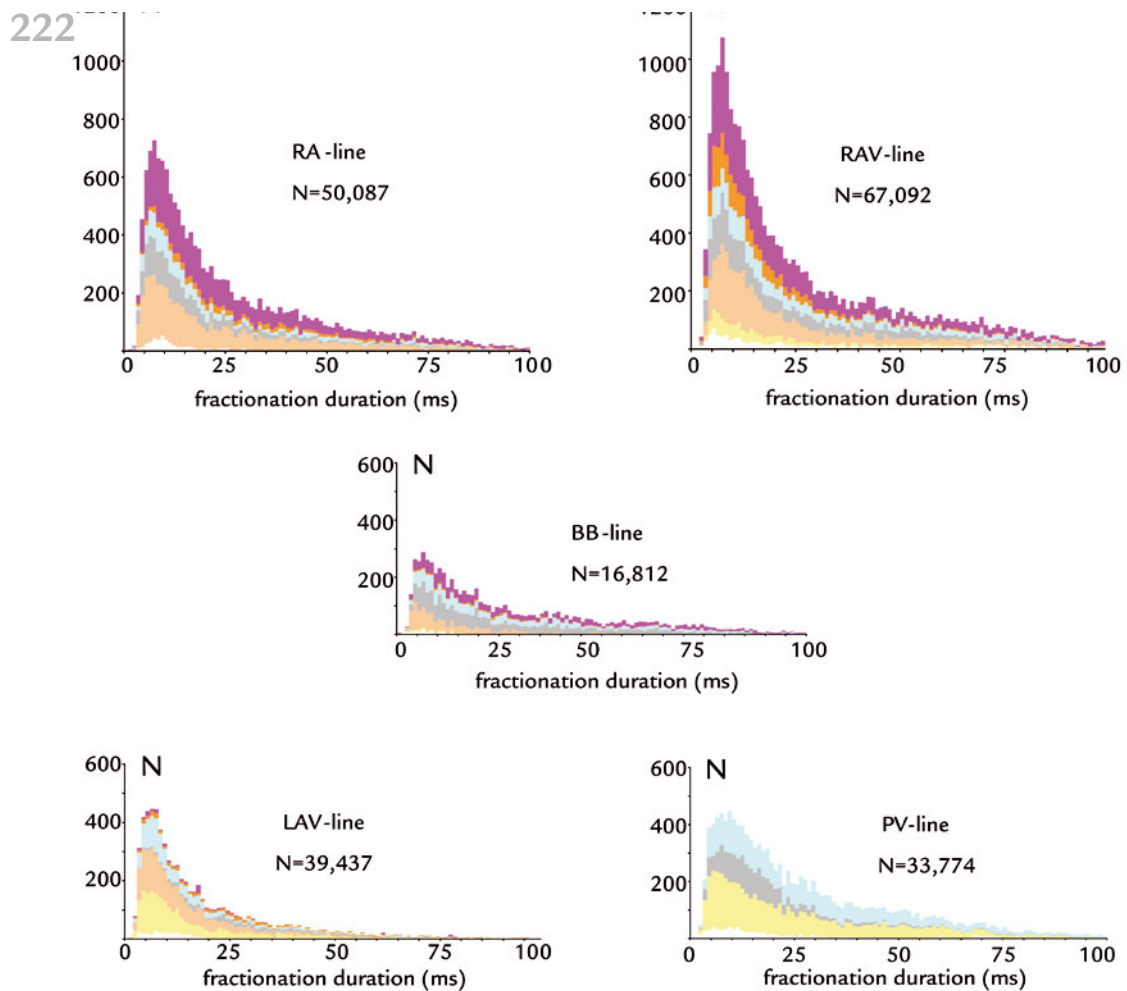


Figure 6. Cumulative relative frequency distribution of fractionation duration of fractionated fibrillation potentials recorded along the different mapping 'lines'. Each patient is again represented by a different color, similar to Figure 3.

averaged degree of fractionation was 17 ± 12 (0-51) %. The incidence of fractionated potentials at the pulmonary vein area was significantly higher than in the right atrium (25 ± 11 (1-40) % versus 17 ± 12 (0-41) %, $p = 0.02$). The intra-atrial variation in the degree of fractionation ranged from 20 to 41 (36 ± 8) %. As demonstrated in Figure 5, there is also an inter-individual variation in the degree of fractionation ($40 \pm 7\%$). Sites with the highest degree of fractionation were found along Bachmann's bundle ($n = 3$), between the pulmonary veins ($n = 2$), at the cavotricuspid isthmus ($n = 1$) and at the posterior right atrial wall ($n = 1$) (lower right panel Figure 5). Sites with the lowest incidence of fractionated potentials were found at the right atrial posterior wall ($n = 2$), Bachmann's bundle ($n = 2$), the left atrioventricular groove ($n = 1$), the cavotricuspid isthmus ($n = 1$) and the left atrial appendage ($n = 1$).

The cumulative relative frequency distribution of fractionation duration of all fractionated fibrillation potentials along the various mapping lines is shown in Figure 6. Each patient is represented by a different color. The averaged fractionation delay of all fibrillation potentials was 23 ± 9 ms. There is no difference in fractionation duration of fibrillation potentials recorded along the RA- (23 ± 8 ms), RAV- (27 ± 9 ms), BB- (20 ± 10 ms) and PV- line (27 ± 10 ms); the fractionation duration of fibrillation potentials recorded along the LAV-line is significantly shorter (17 ± 8 ms, $p < 0.001$). The intra-atrial variation in fractionation duration/fibrillation potential ranged from 21 to 35 (27 ± 5 ms) and the inter-individual variation from 27 to 38 (34 ± 15 ms). Sites with the longest fractionation duration/fibrillation potential were found along the right atrioventricular groove ($n = 2$), the left atrioventricular groove ($n = 1$), at the posterior right atrial wall ($n = 1$), between the pulmonary veins ($n = 2$), or at Bachmann's bundle ($n = 1$). Sites with the shortest fractionation duration/fibrillation potential were found along the right atrioventricular groove ($n = 2$), Bachmann's bundle ($n = 1$), the left atrioventricular groove ($n = 2$), between the pulmonary veins ($n = 1$) and the left atrial appendage ($n = 1$). Thus, apart from an intra-atrial variation in the incidence of fractionated potentials, there were also regional differences in the averaged fractionation duration/fractionated potential (Table 1).

Non-Activated Areas

Figure 7 shows 16 color coded activation maps obtained from the left atrial posterior wall next to the right pulmonary veins, as indicated by the mapping scheme in the lower left corner. These fibrillation maps show a dissociated pattern of activation. Multiple co-existing fibrillation waves, including epicardial breakthrough wavefronts (*), travel over only a small distance before they extinguish. Due to the high incidence of conduction block of fibrillation waves and absence of fibrillation waves activating the other site of the areas of conduction block, parts of the mapping area remained unexcited. The location of these non-activated areas varied from beat to beat. The proportion of activated (white) and non-activated tissue (grey) for every mapping site during 10 seconds of AF is

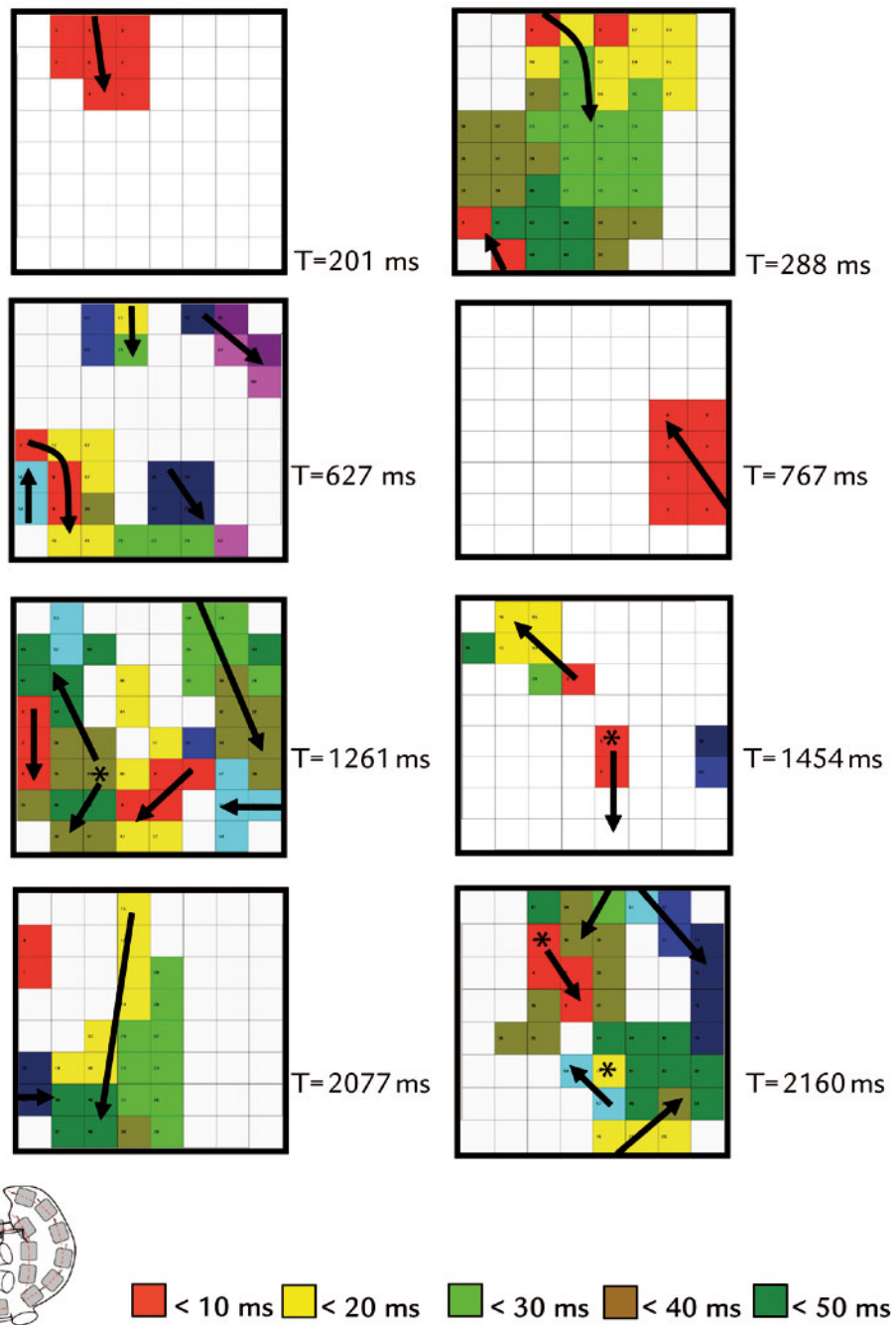
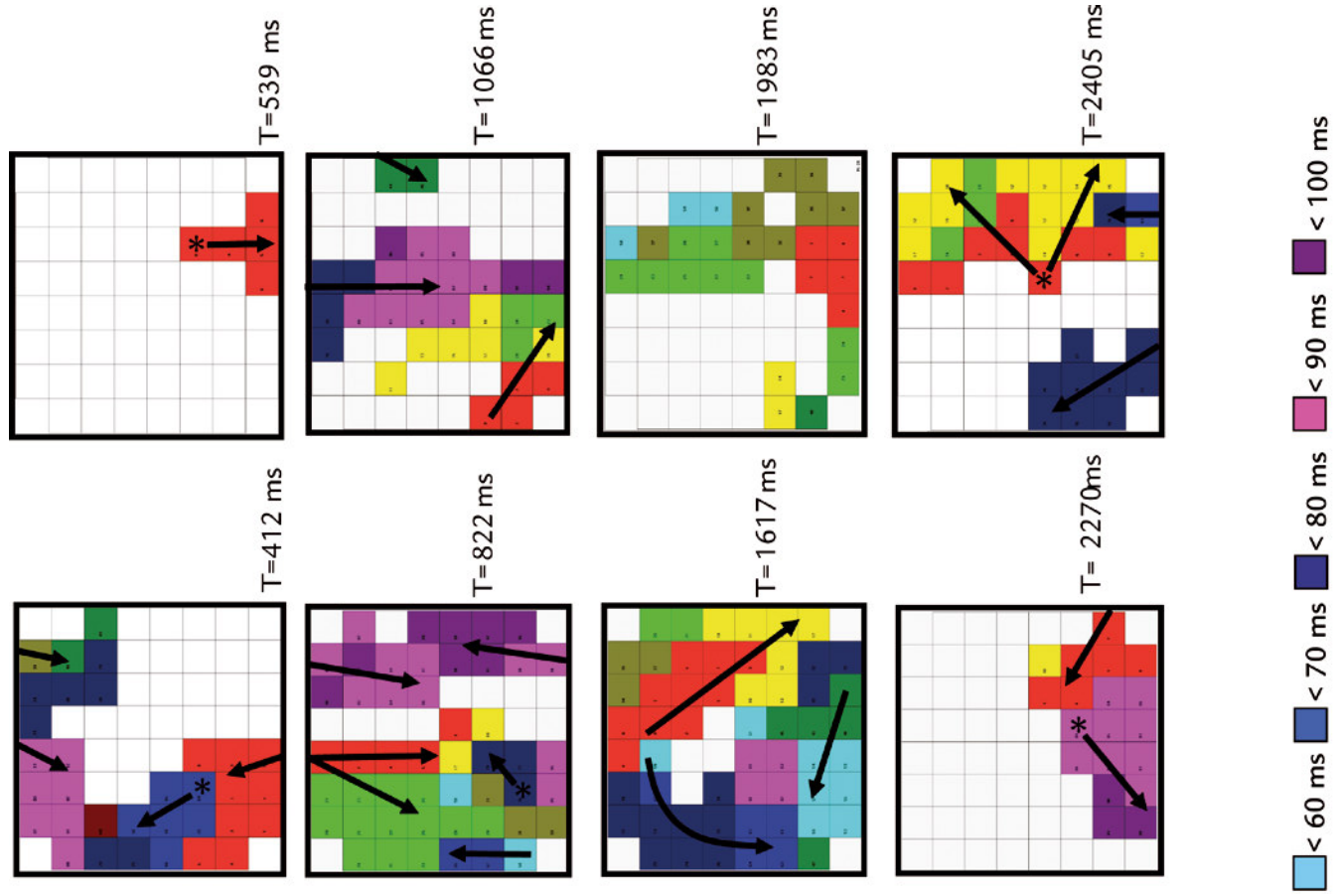


Figure 7.

Sixteen consecutive color coded fibrillation maps constructed from the area next to the right pulmonary veins. Arrows indicate main activation direction. Patterns of activation in this area show a beat-to-beat change in activation direction and multiple epicardial breakthroughs (*). Large parts of the mapping area were not activated due to a high incidence of conduction block of fibrillation waves.



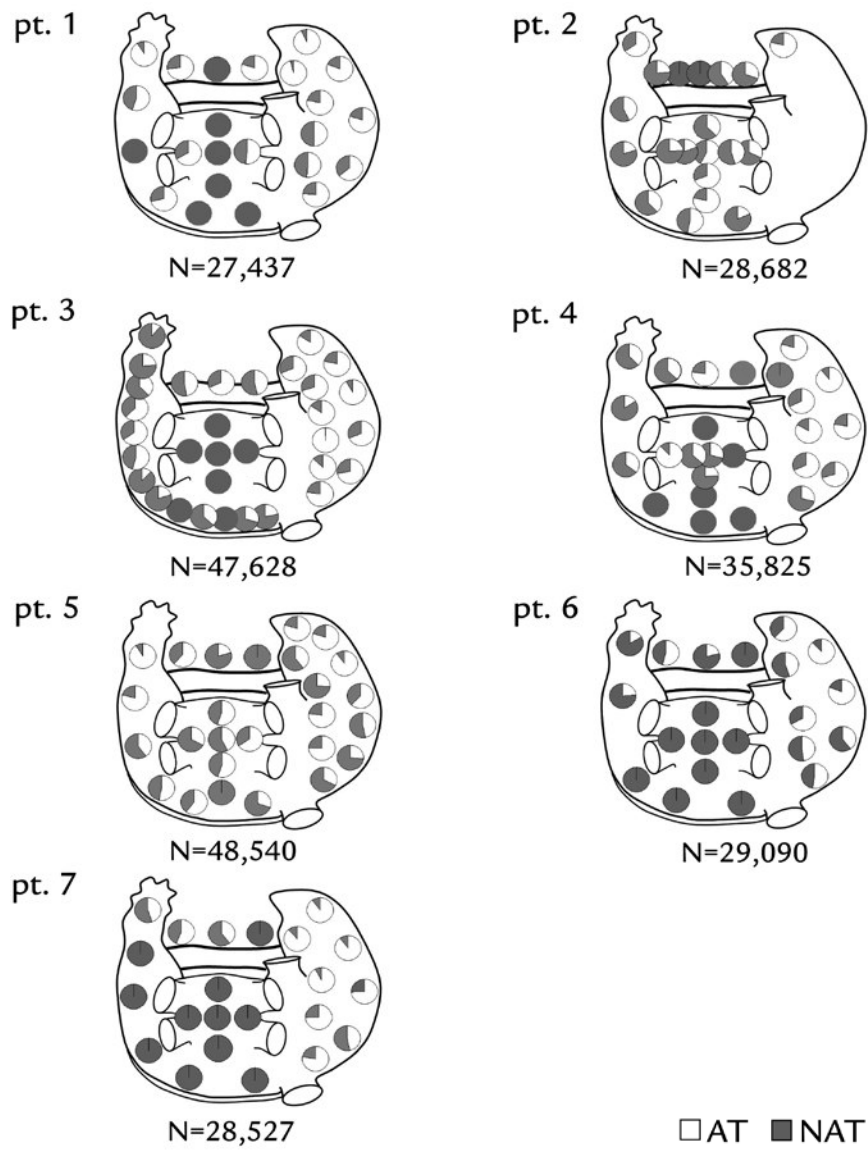


Figure 8. Proportion of activated (white) and non-activated tissue (grey) at every mapping site during 10 seconds of AF. The highest incidence of non-activated areas was found in the left atrium. Dark grey circles represent electrically silent areas. AT = activated tissue, NAT = non-activated tissue.

shown in Figure 8. Comparing the right atrium, left atrium and bachmann's bundle, the proportion of excited tissue was considerable larger in the right atrium ($70 \pm 19\%$ versus bachmann's bundle: $49 \pm 20\%$, left atrioventricular groove: $42 \pm 22\%$, pulmonary vein area: $46 \pm 21\%$, $p < 0.001$). Total electrically silent areas are represented by grey circles.

Conduction Anisotropy and Conduction Block

The intra-atrial variation in conduction block varied from 13% to 25% ($19 \pm 5\%$) and the inter-individual variation in conduction block was $24 \pm 9\%$. There was no difference in the incidence of conduction block along the RA-, RAV and LAV -line (respectively $8 \pm 5\%$, $8 \pm 4\%$ and $6 \pm 6\%$, $p = 0.92$). The highest incidence of conduction block occurred along bachmann's bundle ($13 \pm 11\%$) and the pulmonary vein area ($12 \pm 5\%$, $p = 0.02$).

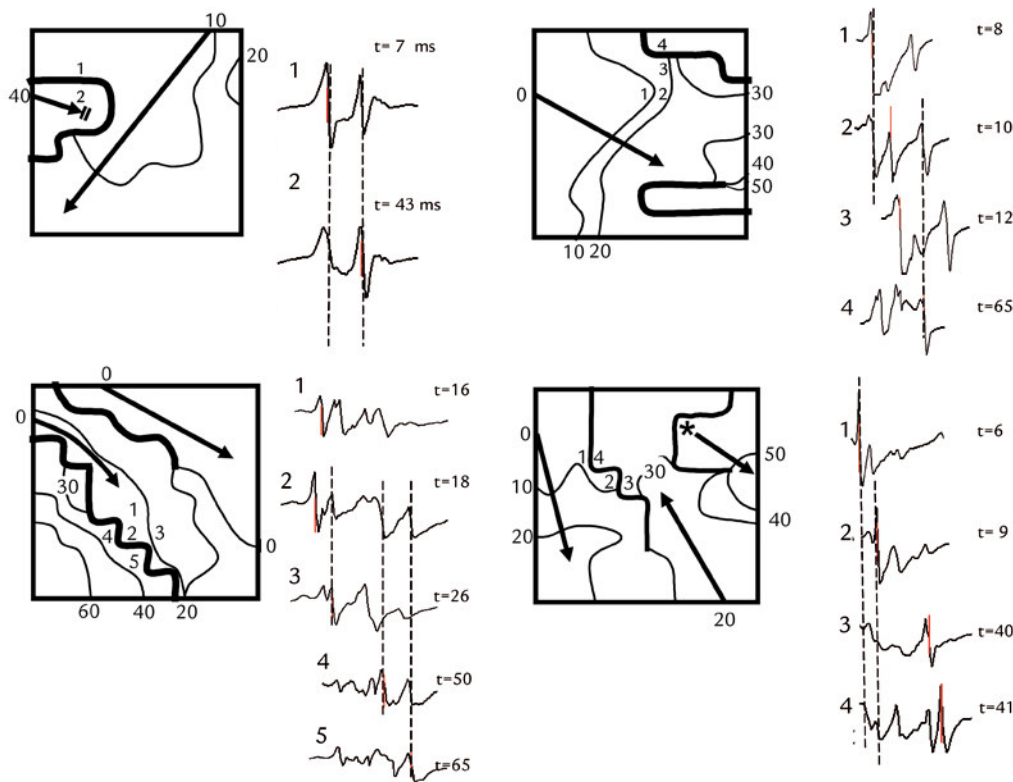


Figure 9.

Relation between spatial patterns of activation and electrogram morphology.

Isochrones are drawn at 10 milliseconds intervals, thick lines represent bi-directional conduction block. Arrows indicate main activation direction. Different components of fractionated fibrillation potentials indicate local asynchronous activation of myocardium around the recording electrode.

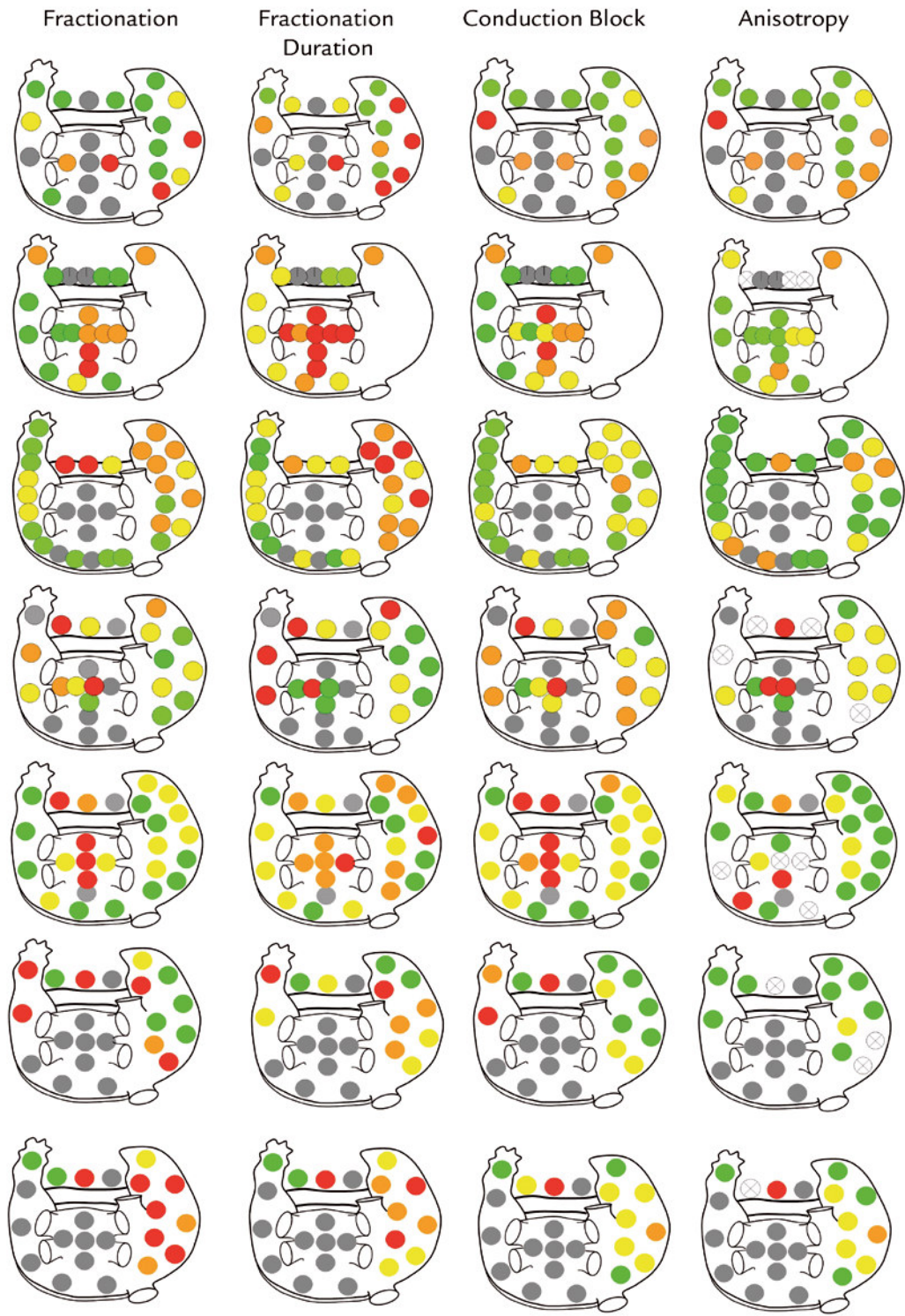


Figure 10.

Color coded mapping schemes demonstrating the relation between the degree of fractionation, averaged fractionation duration/fractionated potential, incidence of conduction block and conduction anisotropy at each mapping site. The magnitude of each parameter is represented by a color ranging from green for the smallest value to yellow, orange and red for the largest values. The strongest correlation was found between the degree of fractionation and conduction block.

Comparable to conduction block, there was no difference in the degree of conduction anisotropy along the RA-, RAV and LAV -line (respectively 1.5 ± 0.29 , 1.45 ± 0.29 and 1.40 ± 0.46 , $p = 0.1$). Regional differences in conduction anisotropy varied from to 1.01 to 2.24 (1.53 ± 0.53). Conduction anisotropy was most pronounced at bachmann's bundle and the pulmonary vein area (1.8 ± 0.63 and 1.72 ± 0.63 , $p = 0.04$). Inter-individual variation in the degree of conduction anisotropy was 1.6 ± 0.55 .

Fractionation and Inhomogeneity in Conduction

Figure 9 shows isochronal maps and long double (upper left panel) and fractionated fibrillation potentials consisting of 3 (upper right panel) and 4 or 5 (lower panel) components recorded within the mapping area. The different components indicate local dissociation in conduction of fibrillation waves around the recording electrode. In chapter 5 we showed that the degree of fractionation was associated with the incidence of conduction block and conduction anisotropy. We therefore analyzed the relation between the degree of fractionation, averaged fractionation duration/fractionated potential, incidence of conduction block and conduction anisotropy at each mapping site. For this purpose, these parameters were quantified for all mapping sites (table1). The magnitude of each parameter is represented by a color ranging from green for the smallest value to yellow, orange and red for the largest values. Results of this analysis are shown in Figure 10. At some areas, conduction anisotropy could not be measured due to preferential conduction directions (white circles).

The incidence of fractionated potentials correlated with the averaged fractionation duration/fractionated potential ($r = 0.56$, $p < 0.001$). The strongest correlation was found between the degree of fractionation and the incidence of conduction block ($r = 0.86$, $p < 0.001$), correlation with conduction anisotropy was less ($r = 0.24$, $p = 0.018$). The averaged fractionation duration/fractionated potential was only associated with the incidence of conduction block ($r = 0.579$, $p < 0.001$) not with conduction anisotropy ($r = 0.12$, $p = 0.25$).

Discussion

Epicardial, multi-site high density mapping of the atria was performed in order to analyze regional differences in the degree and duration of fractionation of fibrillation potentials in patients with CAF. The key finding of this study is that there are large intra-atrial and inter-individual variations in the degree of fractionation, fractionation duration, AF cycle length, conduction block and conduction anisotropy in patients with CAF. These parameters varied considerably over only small distances.

Recent studies showed that ablation of areas of fractionated electrograms eliminated AF thereby suggesting that fractionated electrograms could be used to identify the substrate perpetuating AF.⁵ It is assumed that the arrhythmogenic substrate of AF consists of areas of shorter refractoriness, increased dispersion of refractoriness, heterogeneity in conduction or increased conduction anisotropy, all giving rise to fractionation of fibrillation electrograms.

Regional Differences in Fractionation

Fractionation was quantified during 10 seconds of AF at each site. Surprisingly, most fibrillation potentials recorded at nearly all sites were single or short double potentials. Short double potentials are thought to be the result of transmural dissociation in conduction and are not indicative for abnormalities in conduction.⁶ In all patients, there was a considerable intra-atrial variation in the degree of fractionation. Also, there were large differences in fractionation between closely adjacent areas. Comparing the spatial distribution of fractionated fibrillation potentials between the different patients, the incidence of fractionated potentials at the various atrial sites differed and there were no common predilection sites for fractionation to occur.

Fractionation of fibrillation potentials can be functional and/or structural in nature. In case of multiple, randomly wandering wavelets, it can be expected that the incidence of fractionated potentials is also randomly distributed and that there are no predilection sites for fractionation to occur.

In older patients with mitral valve disease and CAF, it is likely that fractionation is also more structurally determined due to dissociation of muscle bundles by fibrosis or fatty degeneration.⁷⁻¹⁰ If areas of pathological altered myocardium result in fractionation of fibrillation potentials, these areas may be identified by a relative high incidence of fractionated fibrillation potentials. However, sites from which the majority of fibrillation potentials were fractionated were rarely observed in this study population.

Spatial-Temporal Variation in AFCL

Comparable to the degree of fractionation, there was an intra-atrial and inter-individual variation in AFCL. Unexpectedly, fibrillation intervals in the right atrium were shorter than in the left atrium. The longest AFCL was most often recorded from left atrial sites.

In contrast, several experimental and clinical mapping studies have demonstrated that AFCL in the left atrium is shorter than in the right atrium.¹¹⁻¹⁷ Spectral analysis of optical recordings obtained from isolated sheep heart during acetylcholine induced AF found that the shortest AFCL was due the presence of a stable microreentrant source which was most often located in the left atrium.¹⁸ In the right atrium, there was a frequency dependent breakdown of waves resulting in fibrillatory conduction.¹¹ This pattern of activation during AF gave rise to a frequency gradient from the left atrium, across interatrial pathways such as bachmann's bundle or inferoposterior pathways to the right atrium. In addition, it was shown that a shorter AFCL gave rise to a larger variation in fibrillation intervals indicating a higher degree of fibrillatory conduction at faster rates. Recently, Haissaguerre et al. introduced the "Venous Wave Hypothesis".¹⁹ Based on the observation that AFCL progressively increased during pulmonary vein isolation they stated that venous wavelets were the drivers of AF. However, in our study the AFCL around the pulmonary veins was not faster than in the remainder of the atria. Despite the use of high density multi-site epicardial mapping in areas as small as 1.5X1.5 cm we were not able to confirm these findings in patients with CAF. In addition, the absence of a hierarchy of AFCL from the left to the right atria in our study population favors against a left atrial source driving AF in patients with mitral valve disease and CAF.

Electrically Silent Tissue

In most patients, electrical activity was absent in several areas. Electrically silent areas were confined to the left atrium and located along the left atrioventricular groove or the left atrial posterior wall. In one patient, electrical activity was absent in the middle of bachmann's bundle. Absence of electrical activity could be accounted for by replacement of myocardium by fibrotic tissue or fat. Several studies have described histopathological alterations in patients with CAF, including extensive fibrosis and fibro-fatty replacement of the myocardium.²⁰ Interstitial fibrosis in patients with CAF and mitral valve disease particularly occurs around the pulmonary vein area which is consistent with the location of electrically silent areas found in our study.^{21;21}

Examinations of post-mortem hearts have demonstrated that some humans do not have a bachmann's bundle, which could also account for the absence of electrical activity at the middle of bachmann's bundle in some patients.²²

Conduction Anisotropy and Conduction block

The degree of fractionation and fractionation duration correlated with the incidence of bi-directional conduction block; the relation with conduction anisotropy was less pronounced. Though some degree of anisotropy was found, directional differences in conduction velocity were only moderate and not site specific. The anisotropy ratio reported in isolated atrial preparations were much higher, indicating that anisotropy of atrial tissue obtained from CAF patients might be more pronounced at a microscopic scale.¹⁰

Discrepancy between fractionation or fractionation duration and conduction anisotropy could be explained by the fact that anisotropy in this study was measured in relative large areas (3x3 electrodes) compared to measurements of the degree of fractionation. Hence, conduction anisotropy seems a less suitable parameter for identifying the electro-pathological substrate.

Conclusion

232

There are large intra-atrial variations in the degree of fractionation, fractionation duration, AF cycle length, conduction block and conduction anisotropy in patients with CAF and mitral valve disease. These parameters varied considerably over only small distances, suggesting that multi-site high density mapping is essential for accurate identification of the arrhythmogenic substrate.

There were also inter-individual variations in the degree of fractionation at various mapping sites. This supports the hypothesis that there is an inter-individual variation in the location of the arrhythmogenic substrate perpetuating AF.

If ablation of AF is targeted at areas of fractionated potentials, the findings of our study indicates that AF treatment needs to be individualized, which emphasizes the need for a individually based electrogram guided ablation approach. Epicardial multi-site, high density fractionation mapping as presented in this study might therefore become an important tool for identification and subsequent ablation of the arrhythmogenic substrate perpetuating AF in patients with AF undergoing open chest surgery.

References

1. Moe GK, Abildskov JA. Atrial fibrillation as a self-sustaining arrhythmia independent of focal discharge. *Am Heart J.* 1959;58:59-70.
2. Moe GK, Rheinboldt W.C., Abildskov JA. A computer model of atrial fibrillation. *Am Heart J.* 1964;67:200-220.
3. Haissaguerre M, Shah DC, Jais P et al. Mapping-guided ablation of pulmonary veins to cure atrial fibrillation. *American Journal of Cardiology.* 2000;86:9K-19K.
4. Pappone C, Rosanio S, Oreto G et al. Circumferential radiofrequency ablation of pulmonary vein ostia: A new anatomic approach for curing atrial fibrillation. *Circulation.* 2000;102:2619-2628.
5. Nademanee K, McKenzie J, Kosar E et al. A new approach for catheter ablation of atrial fibrillation: mapping of the electrophysiologic substrate. *J Am Coll Cardiol.* 2004;43:2044-2053.
6. Konings KT, Smeets JL, Penn OC et al. Configuration of unipolar atrial electrograms during electrically induced atrial fibrillation in humans. *Circulation.* 1997;95:1231-1241.
7. Kostin S, Klein G, Szalay Z et al. Structural correlate of atrial fibrillation in human patients. *Cardiovascular Research.* 2002;54:361-379.
8. Koura T, Hara M, Takeuchi S et al. Anisotropic conduction properties in canine atria analyzed by high-resolution optical mapping: preferential direction of conduction block changes from longitudinal to transverse with increasing age. *Circulation.* 2002;105:2092-2098.
9. Spach MS. Anisotropy of cardiac tissue: a major determinant of conduction? *J Cardiovasc Electrophysiol.* 1999;10:887-890.
10. Spach MS, Dolber PC. Relating extracellular potentials and their derivatives to anisotropic propagation at a microscopic level in human cardiac muscle. Evidence for electrical uncoupling of side-to-side fiber connections with increasing age. *Circ Res.* 1986;58:356-371.
11. Berenfeld O, Zaitsev AV, Mironov SF et al. Frequency-dependent breakdown of wave propagation into fibrillatory conduction across the pectinate muscle network in the isolated sheep right atrium. *Circ Res.* 2002;90:1173-1180.
12. Harada A, Konishi T, Fukata M et al. Intraoperative map guided operation for atrial fibrillation due to mitral valve disease. *Ann Thorac Surg.* 2000;69:446-450.
13. Jalife J, Berenfeld O, Skanes A et al. Mechanisms of atrial fibrillation: Mother rotors or multiple daughter wavelets, or both? *Journal of Cardiovascular Electrophysiology.* 1998;9:S2-S12.
14. Jalife J, Berenfeld O, Mansour M. Mother rotors and fibrillatory conduction: a mechanism of atrial fibrillation. *Cardiovasc Res.* 2002;54:204-216.
15. Meurling CJ, Sornmo L, Stridh M et al. Non-invasive assessment of atrial fibrillation (AF) cycle length in man: potential application for studying AF. *Ann Ist Super Sanita.* 2001;37:341-349.
16. Nitta T, Ishii Y, Miyagi Y et al. Concurrent multiple left atrial focal activations with fibrillatory conduction and right atrial focal or reentrant activation as the mechanism in atrial fibrillation. *J Thorac Cardiovasc Surg.* 2004;127:770-778.
17. Sueda T, Nagata H, Shikata H et al. Simple left atrial procedure for chronic atrial fibrillation associated with mitral valve disease. *Ann Thorac Surg.* 1996;62:1796-1800.
18. Mandapati R, Skanes A, Chen J et al. Stable microreentrant sources as a mechanism of atrial fibrillation in the isolated sheep heart. *Circulation.* 2000;101:194-199.
19. Haissaguerre M, Sanders P, Hocini M et al. Pulmonary veins in the substrate for atrial fibrillation: the «venous wave» hypothesis. *J Am Coll Cardiol.* 2004;43:2290-2292.
20. Becker AE. How structurally normal are human atria in patients with atrial fibrillation? *Heart Rhythm* 1, 627-631.
21. Corradi D, Callegari S, Benussi S et al. Regional left atrial interstitial remodeling in patients with chronic atrial fibrillation undergoing mitral-valve surgery. *Virchows Arch.* 2004;445:498-505.
22. Platonov PG, Mitrofanova LB, Chireikin LV et al. Morphology of inter-atrial conduction routes in patients with atrial fibrillation. *Europace.* 2002;4:183-192.

